Observations of the late superhump in VW Hydri

van der Woerd, H.; van der Klis, M.B.M.; van Paradijs, J.; Beuermann, K.; Motch, C.

Published in:
Astrophysical Journal

DOI:
10.1086/166521

THE ASTROPHYSICAL JOURNAL, 330:911–921, 1988 July 15

OBSERVATIONS OF THE LATE SUPERHUMP IN VW HYDRI[1]

H. VAN DER WOERD AND M. VAN DER KLIS
Space Science Department of ESA, ESTEC
J. VAN PARADIJS
Astronomical Institute "Anton Pannekoek"
K. BEUERMANN
Institute of Astronomy and Astrophysics, Berlin
AND
C. MOTCH
Observatoire de Besançon
Received 1987 October 29; accepted 1988 January 6

ABSTRACT

We present the results of simultaneous optical and near-IR photometry, optical fast spectroscopy, and *EXOSAT* X-ray observations of the dwarf nova VW Hyi, obtained simultaneously during three consecutive orbital cycles, approximately two days after the 1983 November superoutburst terminated. The optical data show clear evidence for a "late superhump," which is shifted +0.7 in phase relative to the orbital modulation. An attempt is made to derive from the observed spectral distribution the contribution of the late superhump. The orbital hump and the late superhump apparently are not related to each other. This important effect excludes all models, in which the late superhump phenomenon is interpreted in terms of variations in the bright-spot brightness.

Subject headings: stars: dwarf novae — stars: individual (VW Hyi)

I. INTRODUCTION

The defining feature of the SU UMa subtype of dwarf novae is the appearance of optical brightness variations of 6% to 40% amplitude (superhumps) during the long outbursts (superoutbursts). For a recent review of the SU UMa systems we refer to Warner (1985). Vogt (1974), and independently Warner (1975), discovered from photometric observations during the 1972 December superoutburst of VW Hyi that superhumps in this system have a mean period about 3% longer than the orbital period. Early in the superoutburst the superhump has a sharp, pronounced peak with an amplitude of 30%–40% and is clearly asymmetric, with the rise steeper than the decline. During the superoutburst, which typically lasts about 10 days, the superhump amplitude decays to 6%–10%, the period shows an apparent decrease by $\sim 1\%$, and the shape of the superhump becomes broader and more irregular (Haefner, Schoembs, and Vogt 1979; van Amerongen *et al.* 1987).

Near the end of the outburst maximum, approximately within 1 day before the rapid decline toward quiescence, additional peaks appear in the light curve which repeat with the superhump period. One of these peaks remains pronounced during the fast decline and persists for several days after the outburst has terminated. This so-called "late superhump" has about the same period as the superhump observed during outburst maximum, but appears to be shifted by 0.4 to 0.5 in phase with respect to the latter (Haefner, Schoembs, and Vogt 1979; Schoembs and Vogt 1980; Schoembs 1986). Up to now, this late superhump has been observed in VW Hyi, in the eclipsing SU UMa system OY Car (Schoembs 1986), and may have been observed in V436 Cen (Warner 1983).

During quiescence the optical light curve of VW Hyi is normally dominated by an orbital hump of 40% full amplitude. This hump is generally believed to result from obscuration by the optically thick disk or variations in aspect of the bright spot at the outer edge of the accretion disk or both. For about 8 days after a superoutburst, the simultaneous presence of the orbital hump and the late superhump, with their slightly different periods, leads to a beat phenomenon in the optical light curve with a period of almost 3 days (Haefner, Schoembs, and Vogt 1979).

At shorter wavelengths (UV and X-ray) no brightness modulations with either the orbital or the late superhump period have been detected so far. The long integration times (of the order of the orbital period) required to detect VW Hyi during quiescence at a significant signal-to-noise (S/N) ratio prohibit the detection of an orbital modulation. At longer wavelengths (IR) no observations of the late superhump exist.

The late superhump appears to be an essential part of the superhump phenomenon and must be accounted for by any model for the superhumps. In this paper multiwavelength observations of the orbital and late superhump modulations of VW Hyi are presented. We describe the observations in § II. We show in § III that the optical light curve in the various passbands is composed of an orbital hump and a late superhump, which seem to occur without any interdependence. We then give a description of the infrared data (§ IV), the spectrophotometric observations (§ V), and the *EXOSAT* observations (§ VI). The contributions of several possible components to the observed spectral distribution are discussed in § VII. In § VIII we briefly describe the various models for the (late)superhump phenomenon and derive from our data constraints to all these models.

[1] Partly based on observations made at the European Southern Observatory.

II. OBSERVATIONS

Our optical and infrared observations of VW Hyi were obtained 2.5 days after the end of the 1983 November superoutburst, at the European Southern Observatory, La Silla. Four telescopes were used: the ESO 1 m, 1.5 m, and 3.6 m telescopes, and the Dutch 0.9 m telescope. Simultaneous observations in the X-ray band were obtained with the X-ray observatory *EXOSAT*. The journal of observations is given in Table 1.

The ESO 1 m telescope was used for fast white-light photometry (WL). The photometer was equipped with an EMI 6256 photomultiplier tube without filter, and a 16″ diaphragm. The time resolution was 0.5 s. The optical brightness is measured between 3000 and 5500 Å, with an effective wavelength at ~4200 Å. The photometric data were reduced to differential magnitudes with respect to a nearby comparison star.

The Walraven photometer at the Dutch 0.9 m telescope provides simultaneous brightness measurements in five passbands (*VBLUW*), which range between 3200 and 5700 Å (Rijf, Tinbergen, and Walraven 1969; Lub and Pel 1977; see Table 2). The observations were made with an integration time of 8 s, through a 16″ diaphragm. Measurements of the sky background and two nearby comparison stars (CPD −71°250 and CPD −71°252) were made about every half-hour. Extinction correction and a photometric calibration (de Ruiter and Lub 1986) of the brightest comparison star (CPD −71°252) were obtained from observations of four Walraven standard stars. The data were first reduced differentially with respect to this star and transformed to absolute flux F_ν (mJy = 10^{-26} ergs cm^{-2} s^{-1} Hz^{-1}). The brightness and errors (intrinsic and calibration) of the comparison star are given in Table 2.

The infrared data were obtained with the ESO 3.6 m telescope, with an integration time of 40 s. The data were reduced to absolute flux (mJy) using the standard-star observations, made before and after the observations of VW Hyi. The data set consists of observations covering one complete orbital cycle, during which *JHK* observations were obtained in a cyclic way, complemented with 74 minutes of continuous *H* band photometry.

The spectroscopic observations were performed using the ESO 1.52 m telescope, equipped with the image dissector scanner (IDS). The star and sky were observed through two separate apertures of 4 × 4 arsec^2, and their positions were exchanged at regular intervals to allow correction for the different response through the two apertures. Flux calibration was done by observing standard stars several times during the night, and the flat field was obtained from observations of the dome illuminated by a continuum lamp. The wavelength range 4000–7000 Å was covered at a resolution FWHM of 12 Å. Integration times of 1 minute were used throughout, and a total of 127 good spectra were obtained.

TABLE 1

JOURNAL OF THE 1983 NOVEMBER 30 OBSERVATIONS OF VW HYDRI

Telescope	UT	JD Interval[a]	Orbital Cycle[b]	Band
Dutch 0.9 m	0136–0812	0.567–0.842	598.96–602.66	*VBLUW*
ESO 1.0 m	0037–0357	0.526–0.665	598.41–600.28	WL
	0519–0707	0.722–0.797	601.05–602.06	WL
ESO 1.5 m	0146–0210	0.574–0.590	599.05–599.28	IDS
	0236–0353	0.608–0.662	599.52–600.24	IDS
	0529–0616	0.728–0.761	601.14–601.58	IDS
	0702–0727	0.793–0.810	602.01–602.24	IDS
ESO 3.6 m	0213–0357	0.592–0.665	599.31–600.28	*JHK*
	0543–0657	0.738–0.790	601.27–601.96	*H*
EXOSAT LE1	0018–0051	0.513–0.535	598.23–598.54	AL
	0053–0822	0.537–0.849	598.56–602.76	3L

[a] JD minus 2,445,668.0.
[b] Cycle number minus 74,000; the ephemeris is given in the text.

TABLE 2

ABSOLUTE CALIBRATION OF THE COMPARISON STAR CPD −71°252 IN THE WALRAVEN SYSTEM

Band	λ_{eff} (Å)	Width (Å)	log F_ν (mJy)	σ(log F_ν) (mJy)
V	5422	705	2.807	0.004
B	4270	432	2.658	0.008
L	3845	214	2.451	0.015
U	3617	231	2.335	0.015
W	3234	156	2.146	0.015

VW Hyi was observed for almost five orbital cycles with the LE1 telescope, equipped with either the aluminum-Parylene (AL) or 3000-Lexan (3L) filter (7 to 300 Å) and the ME (1.5 to 20 keV) proportional counter array on board the European X-ray observatory satellite *EXOSAT*. These observations were part of a long-term X-ray monitoring program of this dwarf nova during outburst and quiescence, which is described in more detail in van der Woerd and Heise (1987) and in van der Woerd, Heise, and Bateson (1986) and van der Woerd *et al.* (1987).

III. OPTICAL PHOTOMETRY

The overall visual light curve of the 1983 November superoutburst of VW Hyi (Fig. 1 of van der Woerd, Heise, and Bateson 1986) shows that the outburst started in JD 2,445,650. The first superhump was detected at JD 2,445,652.86, 1.6 days after the optical light curve had reached its maximum plateau (Bateson 1984). The outburst lasted until JD 2,445,664, when there was a rapid decline in optical brightness within 2 days to $m_v = 13.0$, followed by a quiescent level between $m_v = 13.0$ and 13.5

The light curve of the fast white-light photometry on 1983 November 30 (JD 2,445,668) is shown in Figure 1. The abscissa marks the orbital cycle ($E - 74000$), where phase 0.0 is defined as the maximum of the orbital hump in the visual light curve, according to the linear ephemeris of van Amerongen *et al.* (1987):

$$\mathrm{HJD(max)} = 2440128.02407 + 0.074271038E \quad \pm 0.00059 \quad \pm 0.000000014\,. \tag{1}$$

The light curve shows a broad maximum, which covers about half the orbital cycle, followed by a rather smooth and narrow minimum. The full amplitude of this modulation is about 50%. A closer inspection of Figure 1 reveals that the maximum seems to consist of two separate peaks; the first one of these changes in intensity from cycle to cycle, but the second one seems to be rather stable. Additional variability on a time scale of minutes is superposed on the maximum. This variability is not coherent (van der Woerd *et al.* 1987). The minimum brightness changes by a few percent from cycle to cycle.

Figure 2 shows the light curve over 3.6 orbital cycles in the Walraven *V* and *U* bands. These light curves also indicate the presence of two peaks at maximum brightness. In the *U* band both peaks are equally strong, whereas in the *V* band the

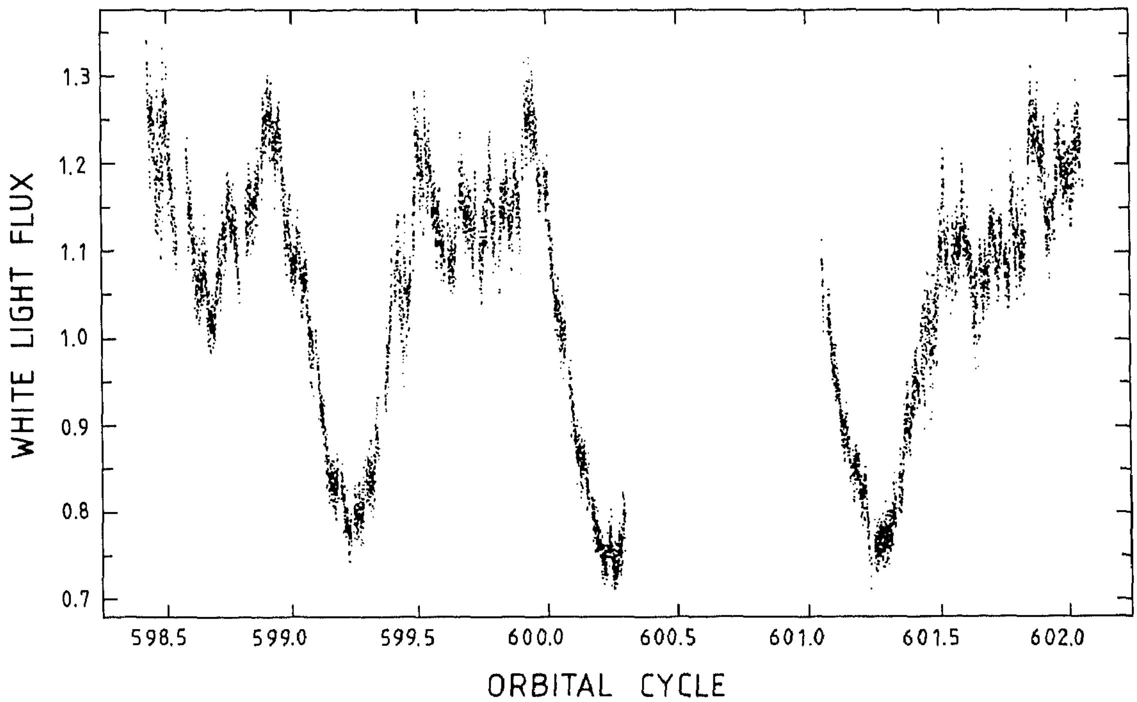

FIG. 1.—The fast white-light photometry obtained on 1983 November 30. The intensity, given relative to a comparison star, is plotted in 2 s bins as function of the orbital cycle. The light curve shows a broad, double-peaked maximum, together with a smooth narrow minimum.

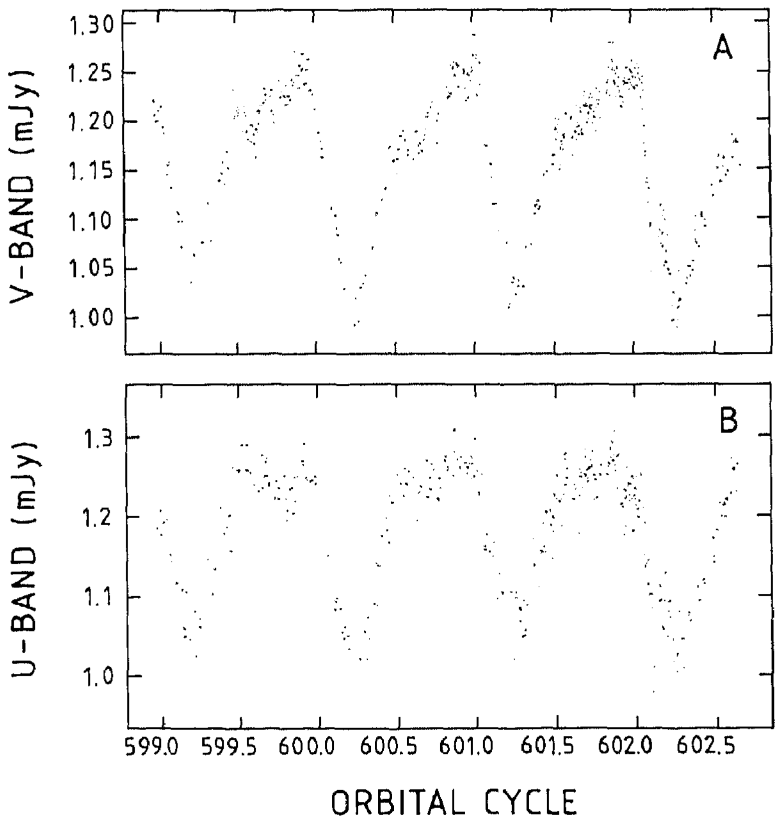

FIG. 2.—The Walraven photometry, covering 3.6 orbital cycles, in (*a*) the *V* band (5442 Å) and in (*b*) the U band (3617 Å). The intensity scale is given in log (mJy).

second peak is stronger than the first one. In other words, the first peak is bluer than the second peak.

The second peak occurs near phase 0.0, i.e., near the maximum of the quiescent orbital hump. Other observations just after a superoutburst seem to indicate that the orbital hump is present at that stage (Haefner, Schoemb, and Vogt 1979). We therefore suspect that the second peak in the optical light curve is mainly due to the orbital hump. We proceed by making the explicit assumption that the observed light curve is a linear superposition of the light curve normally observed during quiescence, plus an extra contribution, whose origin we would like to determine.

The average orbital light curves during quiescence in the five passbands of the Walraven system were determined by van Amerongen *et al.* (1987). These curves, as shown in their Figure 3 (see also our Fig. 3*b*), are quite similar in the five passbands. There is a pronounced hump which shows a fast rise between phases 0.73 and 0.93, followed by the maximum (phase 0.00) and an initially rapid decay till phase 0.2. Hereafter the decay slows down, and the minimum brightness is reached around phase 0.6 (see also Haefner, Schoembs, and Vogt 1979). During quiescence the shape of the orbital hump is known to show variations from cycle to cycle, although the amplitude of the hump remains constant to within 0.05 mag (Haefner, Schoembs, and Vogt 1979; van Amerongen *et al.* 1987).

We have subtracted the mean orbital light curve from our Walraven data. In Figure 3 this subtraction the V band is demonstrated. The upper panel (*a*) shows the observed light curve, in 30 bins per orbital cycle. The middle panel (*b*) shows the mean orbital light curve during quiescence, as determined by van Amerongen *et al.* (1987). The power panel (*c*) shows the observed minus the mean orbital light curve. Figure 3*c* shows that beside the orbital hump component a second component is present, which varies smoothly and has its maximum around orbital phase 0.7.

The subtracted light curves in the five Walraven passbands are depicted in Figure 4. In all passbands the variation is rather symmetric and has an amplitude between 60% and 80%. A sine wave was fitted to these light-curves. In Table 3 we give the best-fit parameters ($\pm 1\ \sigma$) for the period (in units of the

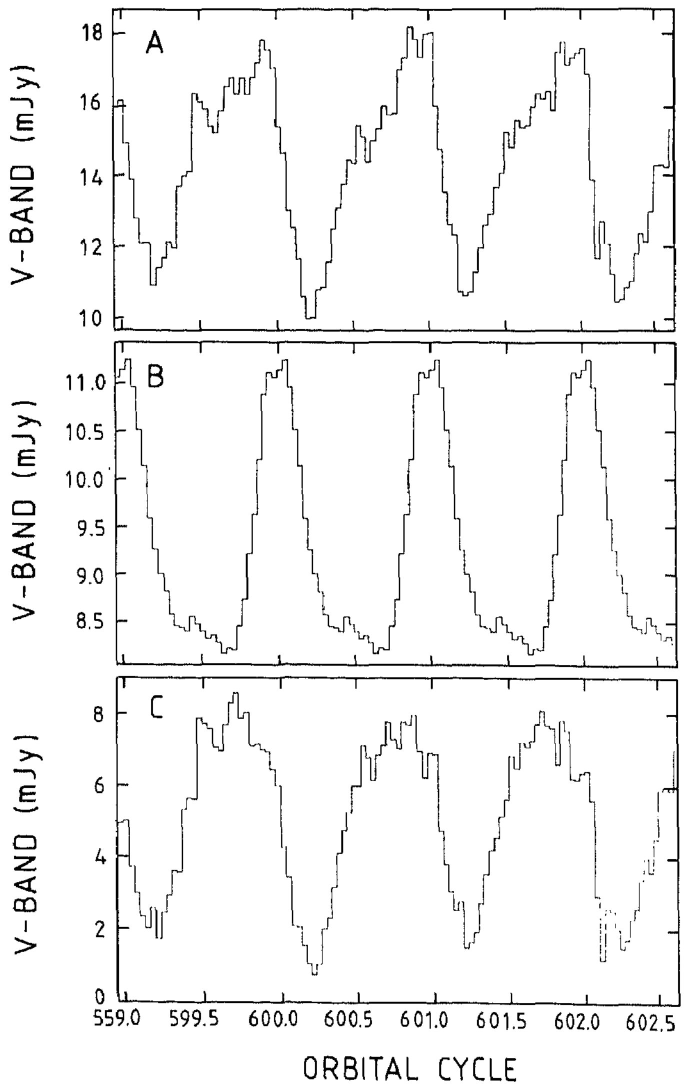

FIG. 3.—An example of the subtraction of the mean orbital modulation during quiescence from the average V band light curve, observed on 1983 November 30. Panel (*a*) shows the average linear V flux curve; (*b*) the mean quiescent orbital modulation, and (*c*) the difference of (*a*) − (*b*).

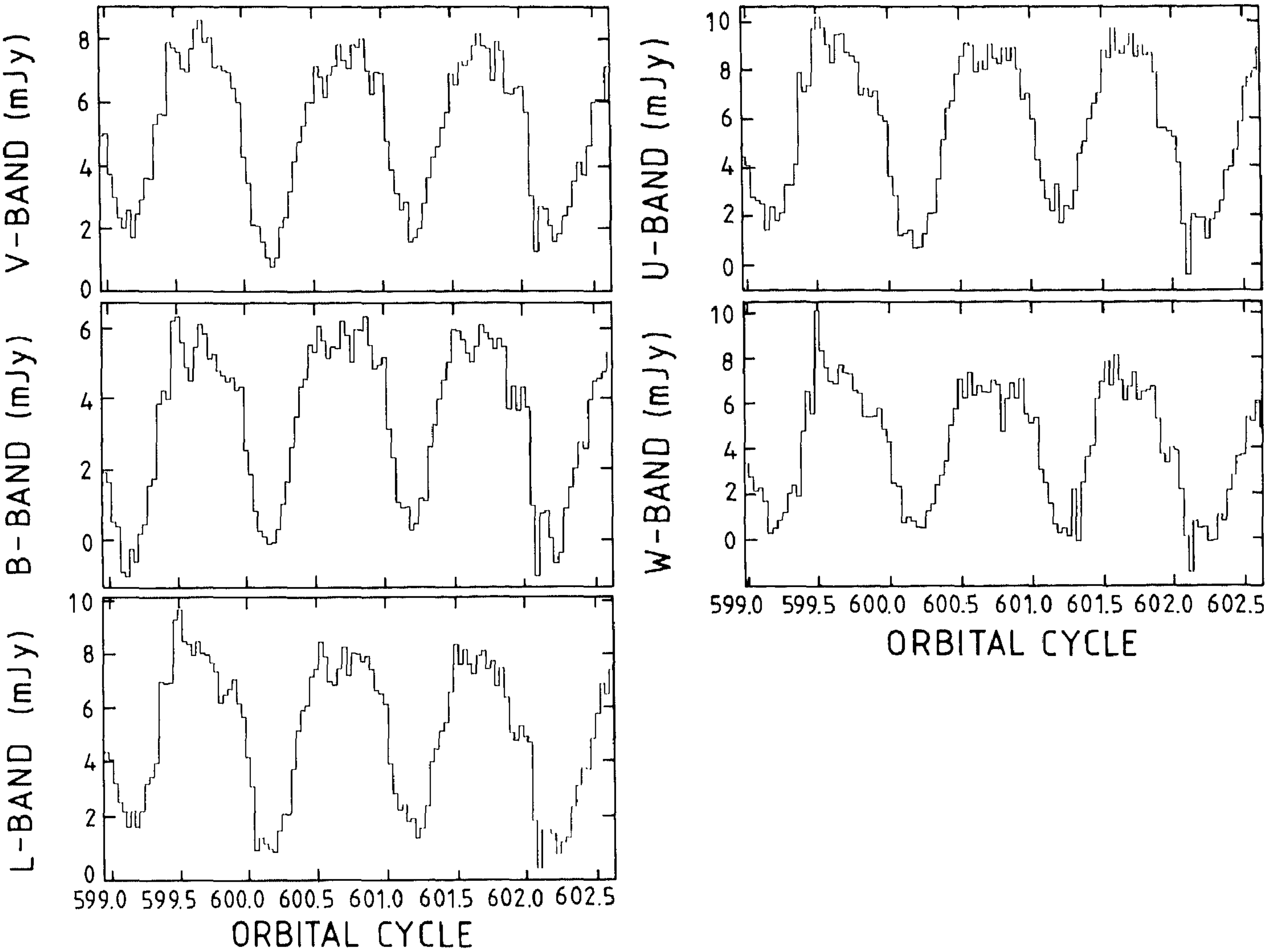

FIG. 4.—The late superhump modulation in the five passbands of the Walraven photometer. Each light curve is obtained by subtraction of the mean quiescent orbital modulation from the data.

orbital period), the mean flux, and the modulation depth (mJy). For comparison the typical orbital modulation during quiescence is given in the last column. An interesting result of the fit is that this component has a period which is 2.5% ± 0.2% longer than the orbital period! This is approximately equal to the superhump period (Warner 1985), and we therefore identify this structure in the light curve with the late superhump.

TABLE 3

PARAMETERS OF THE BEST SINE CURVE FIT TO THE LATE SUPERHUMP MODULATION

Band	Period	Mean	Ampl.(LSH)	Ampl.(ORB)
V	1.024 (0.002)	5.27 (0.03)	2.98 (0.04)	1.33
B	1.024 (0.008)	3.56 (0.10)	2.89 (0.14)	1.45
L	1.029 (0.007)	5.24 (0.10)	3.39 (0.13)	1.23
U	1.024 (0.006)	5.84 (0.10)	3.86 (0.13)	1.23
W	1.026 (0.003)	4.33 (0.03)	3.32 (0.04)	1.18
J	...	25.1 (0.4)	2.9 (0.2)	(0.6)
H	1.068 (0.015)	24.2 (0.3)	2.8 (0.1)	...
K	...	19.9 (0.3)	1.9 (0.1)	(0.6)

IV. INFRARED PHOTOMETRY

The light curve in the H band is shown in Figure 5a. The length of the lines denotes the typical error bar, due to counting statistics. The curve can be described as the sum of a rather sinusoidal variation with a full amplitude of $\sim$5.6 mJy that reaches its maximum around orbital phase 0.9, and a plateau of constant brightness (23.5 mJy) near orbital phase 0.45. The data cannot discriminate between the orbital or late superhump period, although a formal sine fit indicates a period of 6.8% ± 1.5% longer than the orbital period (see Table 3).

In the J and K bands a similar modulation was observed. The values of the amplitudes in all wavelength bands are given in Table 3. These are eyeball estimates, because the short observing time and nonsinusoidal shape of the modulation excluded a good formal fit. The modulation depth (about 10%) is slightly color-dependent, which is shown by the variation of the color index $J-K$ in Figure 5b. The color index is bluer near the maximum brightness of the sinusoidal modulation. The mean value of $J-K$ is 0.72 mag. The mean ratios of the flux (mJy) in the three infrared bands are $H/K = 1.22$ (± 0.02) and $J/K = 1.26$ (± 0.03).

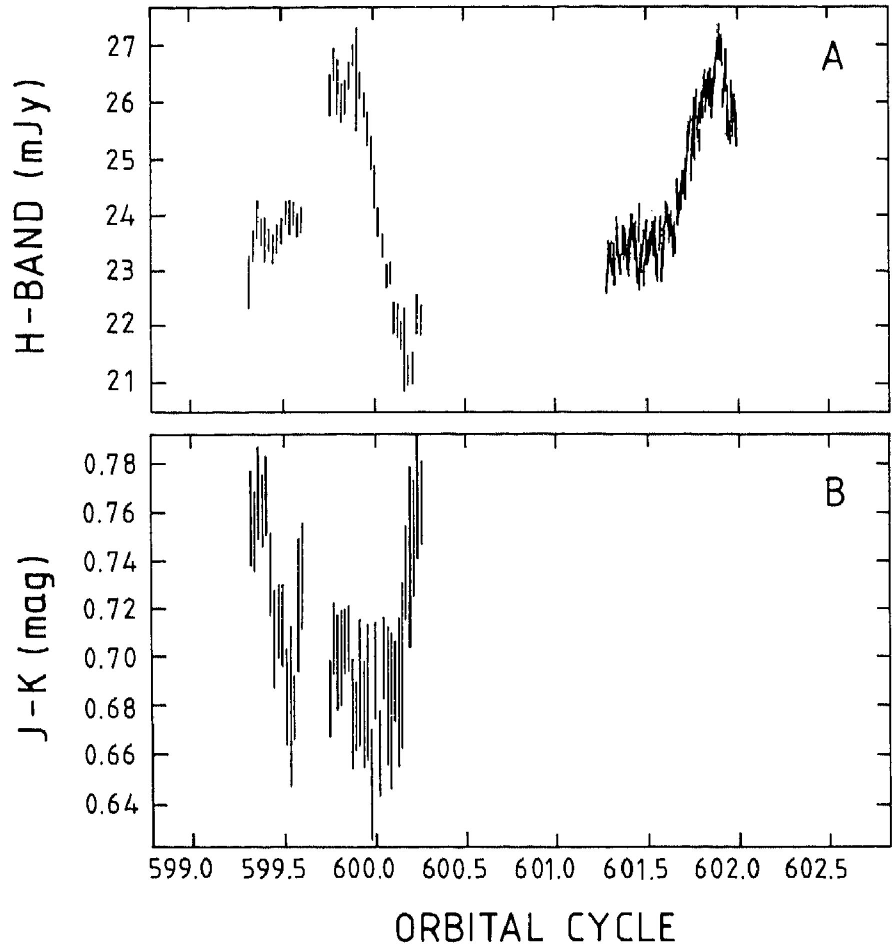

FIG. 5.—(*a*) Light curve of VW Hyi in the H band (1.65 μm). The modulation of $\sim$20% full amplitude reaches its maximum slightly (0.1 in phase) before the maximum of the orbital hump (see Fig. 3*b*). (*b*) Color curve ($J-K$) of VW Hyi during one orbital cycle. The infrared colors are bluer around the maximum of the H band flux.

An earlier observation of the quiescent infrared flux, made in between two normal outbursts (Bateson and McIntosh 1986), is presented in Figure 2 of Sherrington *et al.* (1980). We have divided the data in this figure in phase intervals of 0.1 and analyzed the resulting average light curves in the J and K band. The mean magnitudes are $K = 11.64 \pm 0.05$, $J = 12.61 \pm 0.06$ (both s.d.), and the color index $J-K$ is equal to 0.97 ± 0.04. This corresponds (Johnson 1966) to 13.9 mJy in the K, and 16.0 mJy in the J band. Possibly some variation is present. A sinusoidal wave with the orbital period and maximum at phase 0.0 was fitted to the data and gave a full amplitude of 0.086 ± 0.029 magnitude in the K band. The full amplitude in the J band was 0.078 ± 0.048 mag.

Although orbital modulation in the infrared flux during quiescence can be confirmed only by future observations, it is safe to conclude that this variation will be at most ~ 1.6 mJy in the J and K band, i.e., much less than the 4–6 mJy variation (full amplitude) we observe just after the superoutburst. Therefore the modulation of the infrared flux seems to be connected with the late superhump.

V. SPECTROMETRY

A total of 127 spectra were taken, which cover a complete orbital cycle. In Figure 6 three spectra are shown, which are the average over phase intervals near orbital maximum (1; 0.85–1.05), near late-superhump maximum (2; 0.45–0.65) and at minimum (3; 0.20–0.30) respectively.

The spectra show a blue continuum, superposed on which are strong Balmer emission lines and emission lines from He I ($\lambda\lambda$4922, 5015, 5876, 6678) and Fe II ($\lambda\lambda$4924, 5018, 5163, 5169). In none of the spectra is there an indication of the He II 4686 Å line. Parameters of the emission lines, observed during the rapid decline to minimum (orbital phase 599.096), are given in Table 4. The parameters are derived from simple Gaussian fits. The line center, FWHM, and equivalent width are given in Å. The line intensity is given in 10^{-15} ergs cm^{-2} s^{-1} Å^{-1}.

The emission Balmer decrement is flat. The ratio Hα/Hβ equals 1.37, 1.46 and 1.76 for the spectra 1, 2, and 3 (Fig. 6) respectively. These ratios indicate that the line-emitting region

TABLE 4

EMISSION-LINE PARAMETERS AT ORBITAL PHASE 599.096

Line	Å	FWHM	E.W.	Int.
Hα	6561.33	43.4	38.6	8.12
Hβ	4860.32	40.4	18.0	5.12
Fe II	5169.33	38.3	4.96	1.49
He I	5873.18	60.4	10.6	2.45
He I, Fe II	4923.61	35.3	1.95	0.56
He I, Fe II	5016.40	35.1	3.87	1.14

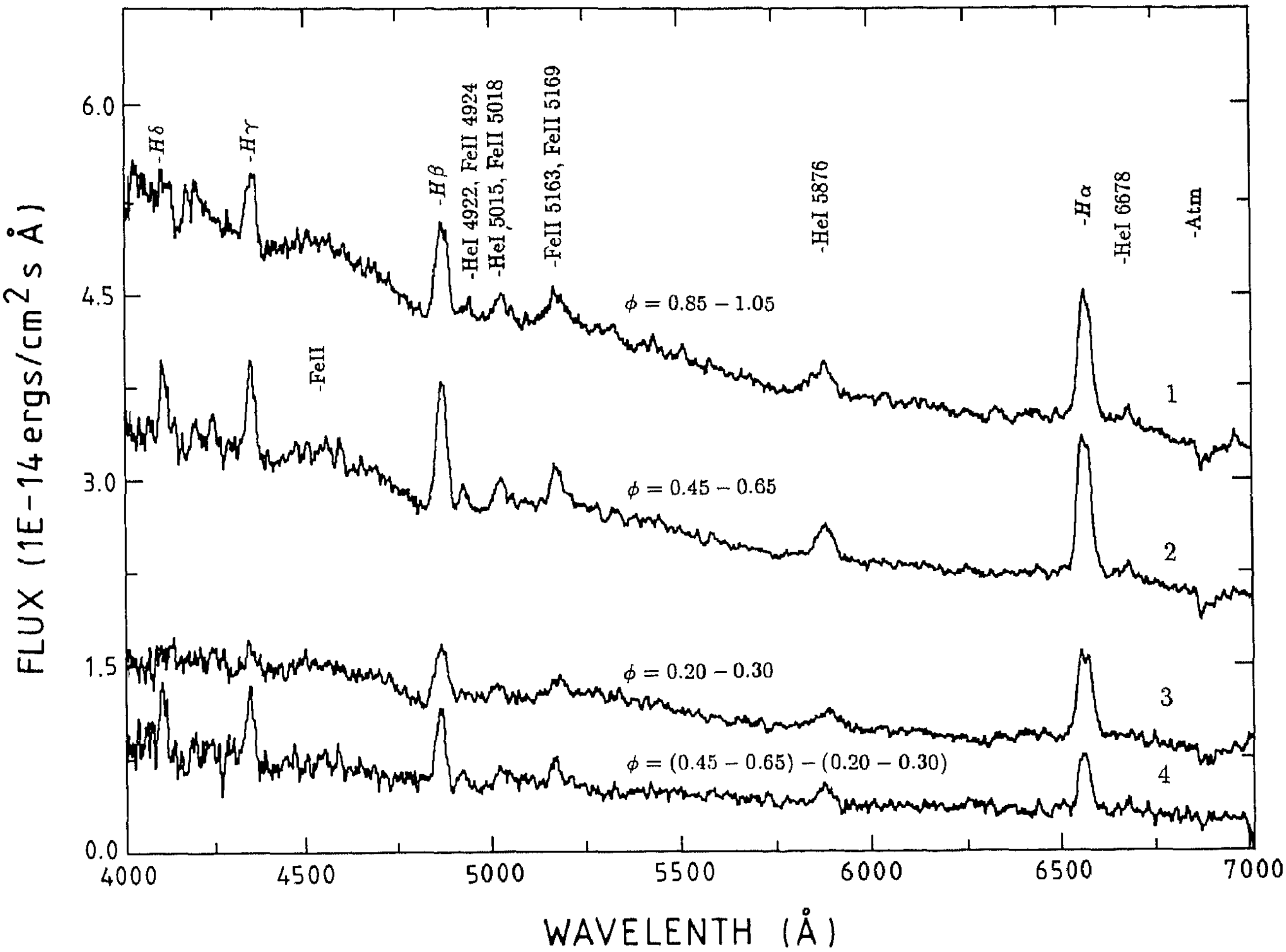

FIG. 6.—Spectra as function of orbital cycle. From top to bottom the curves represent orbital maximum (1; shifted upward by 2 units), late superhump maximum (2; shifted upward by 1 unit), the orbital minimum (3; not shifted) and the residual of curves (2) minus (3), which is representative for the light due to the late superhump modulation (4; not shifted).

is not optically thin in the Balmer lines. The source of the Balmer lines must have an optical depth of 10 or more in the Hα line center, and electron densities in excess of 10^{13} cm $^{-3}$ (Drake and Ulrich 1980). There is a deep depression around Hγ and Hβ which, if interpreted as absorption, corresponds to very large radial velocities ($\sim 10{,}000$ km s^{-1}).

Spectrum (4) is the difference between spectrum (2) and (3), and shows, according to our basic assumption, the spectrum of the late superhump modulation. The continuum flux is flat in F_ν versus ν. The late superhump light is not optically thin in the Balmer lines (Hα/Hβ = 1.05) and does not show the depressions around Hβ and Hγ.

The Hα emission line has a very complex structure. Visual inspection of the line profile as function of orbital phase did not reveal any clear trend. Some spectra clearly show a double-peaked Hα line. The typical separation between the two peaks is ~ 1000 km s^{-1}.

Fits to the Hα line in the individual spectra were made with a single Guassian profile. The result of these fits, given as average values in 10 phase bins, are shown in Figures 7*a–d*. In these figures the average value and best-fit with a sine curve are drawn. Note that the 1 σ of the distribution, and not the mean error, is plotted. In view of the complex structure of the Hα line these curves must be regarded as an indication of the overall varition of the line parameters with the orbital or late superhump period.

The derived mean systematic velocity is $\gamma = -75$ (± 11 m.e.) km s^{-1}. The radial velocity curve has a half amplitude of $K = 88$ (± 16 m.e.) km s^{-1}and reaches a maximum value toward the observer at orbital phase 0.5 (Fig. 7*b*). This is consistent with previous spectrometric results, also obtained 2 days after the end of a superoutburst (Schoembs and Vogt 1981). Whether these values, derived from a single Guassian fit to the lines, reflect the radial velocity curve of the line-emitting region can only be answered when we have a better understanding of the origin of the complex structure of the line itself. The equivalent width of the line reaches a maximum at phase 0.5 (Fig. 7*a*), while the maximum intensity is reached 0.2 later in phase (Fig. 7*d*), i.e., near the maximum of the late superhump continuum flux. The FWHM (Fig. 7*c*) shows the opposite behavior of the line intensity; the width is at a minimum near orbital phase 0.7.

VI. X-RAY PHOTOMETRY

The *EXOSAT* observations showed that the accretion onto the white dwarf had returned to a level typical of the quiescent state. The count rates in the LE1 (3000 Lexan filter: 0.0276 ± 0.0016 counts s^{-1}; al-Pa filter 0.0120 ± 0.0054 counts

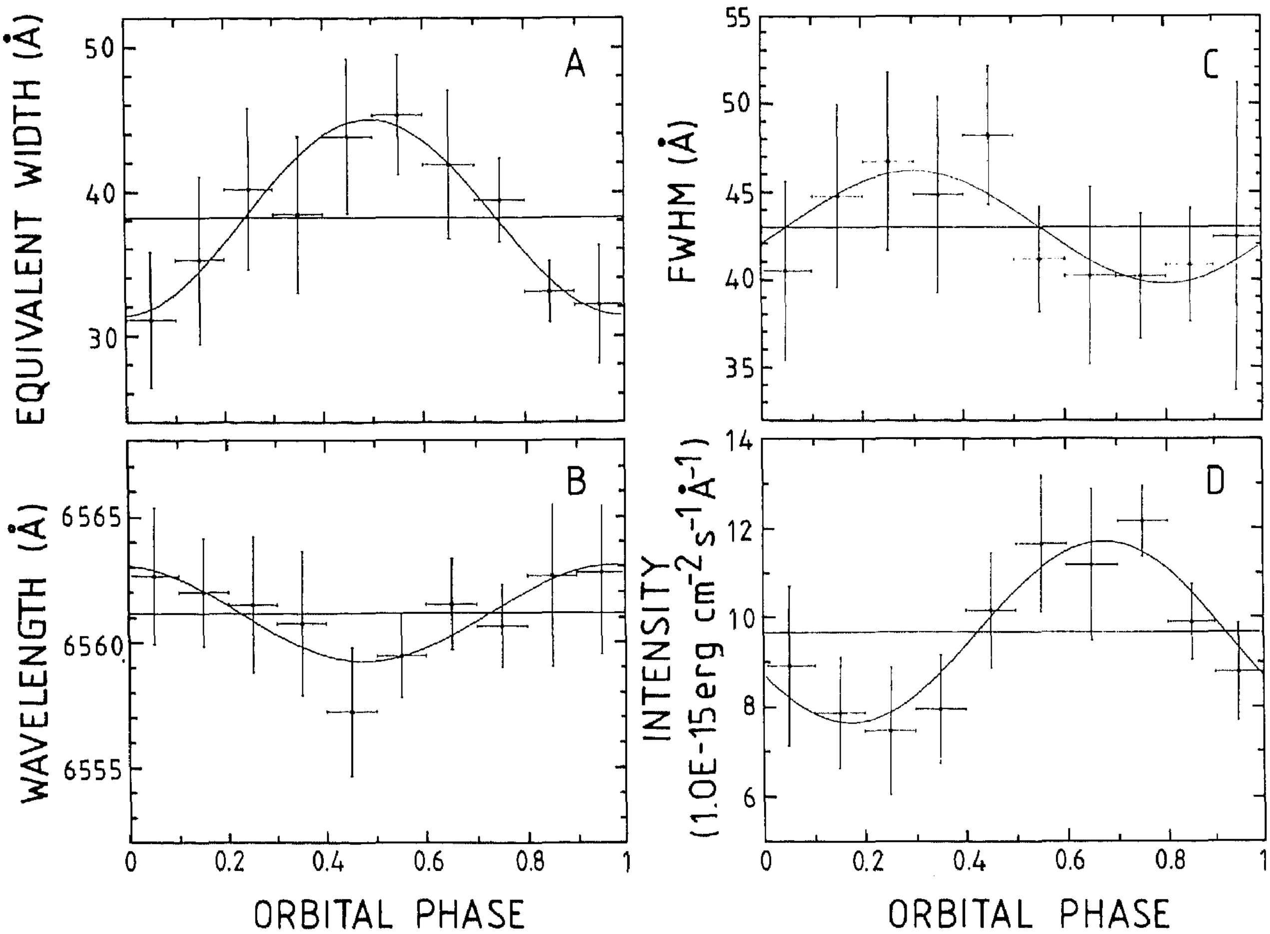

FIG. 7.—The line parameters of Hα, as function of orbital phase. The horizontal error bar indicates the phase bin, the vertical error bar gives the 1 σ error. The average value and best sine-curve fit are plotted.

s^{-1}) and ME (0.240 ± 0.044 counts s^{-1} for the Half 1 detector array in the 1 to 6 keV band) are consistent with a bremstrahlung spectrum of $T \approx 10^8$ K, which emits a total flux of 10^{-11} ergs cm^{-2} s^{-1} (van der Woerd and Heise 1987).

The system was observed for almost five orbital cycles. No variation in the X-ray flux with orbital or late superhump period was detected at a level above 19% (99% confidence). From a long exposure at 1984 May 1 (8.5 orbital cycles) an upper limit of 10.9% can be set to the orbital modulation in the LE1 3000-Lexan flux during quiescence.

VII. SPECTRAL ANALYSIS

In the previous sections we have analyzed the light curves of VW Hyi in various passbands and in the emission lines and tried to extract from these curves the variations due to the late superhump modulation. In this section we will tie together the spectral information on the late superhump. We will discuss the data in order of increasing wavelength.

The X-ray flux is no different from other quiescent observations and shows no strong modulation with the superhump period, which indicate that the accretion process near the white dwarf is not greatly influenced by the late-superhump phenomenon. This can also be derived in the following way: it has been suggested by Mateo and Szkody (1984) that most of the UV flux of VW Hyi comes from a hot white dwarf with a temperature of $T = 18{,}000 \pm 2000$ K. They reached this conclusion from the presence of a turnover in the quiescent spectra at $\lambda \approx 1400$ Å, which they interpreted as the high-gravity pressure-broadened Lyman-α line of the white dwarf. Our spectra (Fig. 6) do show broad absorption features near Hγ and Hβ, which may be very broad Balmer lines in absorption, coming either from the white dwarf itself (pressure broadening) or from the boundary layer (pressure and Doppler broadening). From the depression around Hβ, we find that it is not implausible that a high-gravity atmosphere contributes 30%–40% to the light at this wavelength (Wesemael *et al.* 1980). According to this interpretation, the absence of the absorption features in the late superhump spectrum (Fig. 6, spectrum 4) would indicate that the late superhump light is not coming from near the white-dwarf surface. However, the decrease of the UV flux during quiescence, with 20%–30% within 30 days, appears inconsistent with the idea that all UV flux is coming from a hot white dwarf. We refer to the paper by Pringle *et al.* (1987) for a discussion on this topic.

The late superhump variation has an amplitude of ~3 mJy in the Walraven passbands. This variation is larger in the *U* and *W* band (which lie below the Balmer jump) than in the *V* band. This is an indication that the Balmer jump is in emission, and that therefore part of the late superhump flux in the Walraven bands originates from an optically thin plasma. This follows also from the analysis of the emission lines. Figures 7*c*, *d* indicate that around orbital phase 0.7, at the maximum of the late superhump, the Hα line may possibly have a narrow intense component.

It is crucial to find out whether the variation in the near-infrared is to be attributed to the orbital hump, to the companion star or to the late superhump. The color temperature of the orbital hump modulation, as derived from the variation in the Walraven bands, and from the absence of a clear modulation in the *IUE* wavelength range, is of the order of 11,000 ± 2000 K (Pringle *et al.* 1987; Mateo and Szkody 1984). From this temperature and the observed orbital variation in the Walraven bands, we expect an orbital variation of ~0.6 mJy in the infrared J band, which is close to the modulation depth in the quiescent data of Sherrington *et al.* (1980), but much less than the variation of 2.9 (±0.2) mJy in our J band data. Generation of the infrared modulation by an optical thick source should therefore require a temperature lower than 11,000 K of the orbital hump. Therefore this modulation is either not coming from the late superhump (which has a higher color temperature than the orbital hump) or the source is not optically thick.

There are two reasons to believe that most of the infrared light is not generated by the red dwarf, unless the radiation of this star is strongly modified, e.g., by the previous super-outburst. First, the infrared light seems to vary with approximately the orbital period. If most infrared light comes from the companion star we expect a variation with half the orbital period, due to the tidally and rotationally induced ellipsoidal variations (Berriman *et al.* 1983). Second, the companion star in VW Hyi, with a short orbital period of 1.7825 hr, is expected to be of late spectral type (M5/M6) and to be very cool ($T = 3000 \pm 150$ K); see Patterson (1984). The $(J-K)$ color index for such a star ranges between 0.89 and 0.95 (Johnson 1966). Direct evidence for the presence of this type of cool companion stars has come from infrared observations of eclipsing SU UMa systems (Bailey *et al.* 1981; Berriman 1984). The observed color index $J-K = 0.72$, is characteristic of a K7/M0 dwarf with a temperature of ~4000 K. If we approximate the stellar atmosphere by a blackbody source with this temperature, we find that it should have a radius 2.18 (d/100 pc) times the radius of the companion star (1.25×10^{10} cm). Therefore the companion star cannot generate all the observed infrared flux, unless VW Hyi is closer to Earth than 46 pc.

If, on the other hand, the observed infrared flux would come from a flat disk, seen under an inclination of 60° (Schoembs and Vogt 1981) and with a temperature of $T \approx 3800$ K, this would imply a disk radius of 3.09×10^{10} (d/100 pc) cm, i.e., this cool material would fill a large fraction of the accretion disk, which has a radius of $\sim 3 \times 10^{10}$ cm.

The fact that emission of the infrared light by an optically thick component in dwarf nova systems (blackbody or stellar atmosphere) systematically gives very large extensions for the infrared source led Berriman, Szkody, and Capps (1985) to the conclusion that much of the infrared light must come from an optically thin source. The basic idea is that, although an optically thin plasma is a less effective radiator than a blackbody, the infrared flux can come from a much hotter plasma, which results in a smaller volume of the source. Berriman, Szkody, and Capps (1985) suggested that the source of infrared light is similar to that required to support the Balmer emission lines, which would imply a temperature of order $1\text{–}2 \times 10^4$ K.

This, in fact, is not a bad idea. An optically thin plasma with these temperatures emits a spectrum that is rather flat in F_ν versus ν; this would give a natural explanation for the 2 to 3 mJy variation in the infrared and Walraven bands. The emission measure, as derived from the broad-band measurements, is of the order of 10^{56} cm^{-3} (Ferland 1980). From the ratio of the Balmer emission lines we had already derived that the electron density is 10^{13} or more, which implies a volume of less than 10^{30} cm^3; e.g., for an electron density of 10^{14} cm^{-3} the radiation volume comprises ~1% of the accretion disk.

In summary, our basic assumption that the observed flux is a linear superposition of the average orbital modulation plus the late superhump modulation leads to a consistent description of the source of the late superhump flux: the source is optically thin in the continuum and optically thick in the Balmer emission lines, which contributes to the optical-continuum, optical-line, and infrared emission.

VIII. (LATE) SUPERHUMP MODELS

The above given analysis has shown that the observed light curve can be described by a linear superposition of the orbital modulation and a late superhump modulation. Also, previous observations of the system VW Hyi have shown that these two phenomena can be present, apparently without any interdependence (Haefner, Schoembs, and Vogt 1979; Schoembs and Vogt 1980). Furthermore, the assumption that the orbital modulation is essentially similar to that observed during normal quiescence resulted in a consistent description of the late superhump modulation. Therefore the hot-spot brightness and its varation with orbital phase seem not to be influenced by the presence of the late superhump. This observational result does not fit within any of the theoretical models for the late-superhump, proposed so far.

These models include (1) a hot "starspot" on an asynchronously rotating secondary; (2) modulation due to a strong magnetic field of the slowly rotating white dwarf; (3) periodic mass-transfer modulation through the inner Lagrangian point; (4) a massive elliptical ring around the accretion disk; and (5) tidally induced deformation of the accretion disk. We give a short summary of the basic features of each model, with particular emphasis on interpretation of the late superhump. A more general discussion on the observational constraints to the models can be found in the works of Patterson (1979), Vogt (1982), and Warner (1985).

1. Whitehurst, Bath, and Charles (1984) concluded, based on eclipse observations of Z Cha during superoutburst, that the superhump light is not eclipsed, and proposed that the superhumps originate from the eclipsing component; i.e., the red companion star. However, Smak (1985) disagreed and concluded that the additional source of light responsible for the superhump in this system undergoes a partial eclipse, which would locate its origin in the vicinity of the accretion disk (see also Horne 1984). In this model the orbital and late superhump have no direct relation. However, the appearance of late superhumps near the end of the superoutburst, out of phase with the superhump, would require the unexplained formation of a secondary hot spot on the red star.

2. Warner (1985) proposed that a beam of X-ray and UV radiation from a weakly magnetized white dwarf illuminates the disk, analogous to the situation in intermediate polars. Rotation of the white dwarf with the beat period (typically 3 days) would result in a variation (with the superhump period) of the illumination of the disk, notably in the region of the hot spot. The late superhumps are thought to orginate from the second magnetic pole, which only becomes visible at the end of a superoutburst (Warner 1985). It remains unclear, however,

why the accretion on the "superhump" pole should suddenly switch off. A further argument against this model is given by the discovery of a 15.9 minute optical oscillation in the SU UMa system SW UMa, which is interpreted as the rotation period of the white dwarf (Shafter, Szkody, and Thorstensen 1986). Finally, in the case of VW Hyi, the extensive set of X-ray observations shows that radial accretion onto the white dwarf, as in intermediate polars, is highly unlikely (van der Woerd and Heise 1987).

3. According to Papaloizou and Pringle (1979) the superhump is due to variability of the hot-spot brightness. These are caused by mass-transfer variations, triggered by a slight eccentricity ($e \approx 10^{-3}$) of the binary orbit (see also Clarke, Mantle, and Bath 1985). It is not clear whether the required value of the eccentricity can be maintained, and why the mass-transfer modulation at the inner Lagrangian point would undergo a phase shift of half a cycle shortly after the superoutburst. The strongest objections to this model come from the radial velocity variations observed in Z Cha during superoutburst (Vogt 1982; Warner 1985).

4. According to Vogt (1982) superhumps are due to the changing brightness of the hot spot, resulting from the presence of an eccentric ring of material around the disk, but within the primary's Roche lobe. The long axis of this eccentric ring is assumed to revolve by apsidal motion, in the observer's frame of reference, with the beat period (~ 3 days) between the orbital period and superhump period. The impact of the mass-transfer stream with this eccentric ring occurs at varying distances from the white dwarf; this results in a modulation of the hot-spot brightness due to the varying kinetic energy of the impact stream. In this model the superhump maximum occurs when the bright spot is located at periastron (relative to the white dwarf) of the elliptic ring, when the mass-transfer stream reaches deepest into the potential well. One of the unsolved theoretical problems for this model is whether the ring can persist for more than 100 orbital periods, as observed in VW Hyi (Whitehurst 1984; Hensler 1985). A strong observational argument against this model is that the bright spot appears to remain at almost the same radius vector than that occupied during the quiescent state (Warner 1985). Vogt (1983) makes the ad hoc assumption that matter, which would have been expelled during the superoutburst, would interact with the companion star at the outer Lagrangian point L_3 and so give rise to the late superhumps.

The superoutburst model proposed by Osaki (1985) is, in a sense, a combination of models (3) and (4). According to this model the superoutburst is due to increased mass transfer, which is the result of heating of the secondary's atmosphere by irradiation from the vicinity of the white dwarf. The amount of irradiation, and thereby the mass-transfer rate, is modulated by the obscuration of a slowly precessing eccentric ring at the outer disk. Osaki (1985) proposes that near the end of the superoutburst, when the mass-transfer rate has dropped back to approximately the quiescent rate, the eccentric ring survives for about 1 week. Therefore the bright-spot brightness will still vary periodically with the superhump period as before because of the varying potential energy at the impact point. There are some arbitrary assumptions within this model, like the azimuthal variation of the vertical extension of the eccentric ring, which determines the amount of irradiation, and the mass-transfer reaction time of the secondary to irradiation. A fundamental problem for this model is that during outburst the X-ray spectrum is much too soft (van der Woerd and Heise 1987) to influence the energy balance within the secondary's photosphere, and thereby the mass-transfer process (Hameury, King, and Lasota 1985).

5. Recently, Whitehurst (1987) proposed that the tidal action of the companion star can induce a resonance effect in the accretion disk. A slowly (3 days) precessing elongated disk is thereby formed during outburst. In this model the superhump modulation is caused by a periodic variation in the viscous dissipation within the disk; the superhump light reaches a maximum when the tidal shears are strongest. Whitehurst claims that the time of growth of this resonance effect is of the order of a few days, which makes it only observable in the (long) superoutburst. Whitehurst (1987) reports that the dissipative process, which causes the superhump modulation during superoutburst, does not work efficiently during quiescence. Also in his model the late superhumps originate from the interaction between the mass-transfer stream and a slowly decaying eccentric disk, i.e., a varying bright-spot brightness as in the Osaki model.

We may summarize this description of the superhump and late superhump models by concluding that none of the models can fully explain all observational aspects. Indeed the models (1) to (4) have already severe problems with observations of the superhumps. The models of Osaki and Whitehurst encounter less problems, and seem therefore the best alternatives. Both models attribute the late superhump modulation to a varying depth of the bright-spot position in the potential well.

Our observations contradict this picture. From Figure 3 it appears that the late superhump modulation in the V band is almost a factor of 2. If this is to be attributed to a changing depth in a $1/r$ potential, it implies an eccentricity of the outer rim of the disk of $e \approx 1/3$. First, this is a large value on dynamical grounds and would be difficult to maintain for at least 2 days after the superoutburst. Second, the mass-transfer stream is expected to change drastically in orbital position, and the orbital hump modulation should be different, and shifted in phase compared to the normally observed orbital modulation.

It is well known that the source of superhump modulation is only slightly affected by the orbital modulation (e.g., Haefner, Schoembs, and Vogt 1979). Only in the high-inclination and eclipsing systems Z Cha and OY Car the superhump brightness shows partial eclipses (Smak 1985), and a modulation with the beat period, i.e., a weak correlation with the orbital phase of the superhump (Warner 1985; Schoembs 1986). These aspects indicate a location for the superhump source within the accretion disk. They do not, however, connect in any way the superhump with the point of interaction between accretion disk and mass-transfer stream. This is a strong point in favor of the Whitehurst (1987) model for superhumps.

We claim also that the late superhump modulation is not related in any sense to the mass-transfer process, but originates from within the accretion disk itself. In § VII we have presented evidence that the bulk of the late superhump emission comes from an optically thin plasma. The modulation of this emission can either be due to a partial obscuration of the source, or to a modulation of the energy dissipation. The second possibility could be due to a remnant of the tidal distortion of the accretion disk, as proposed by Whitehurst (1987).

IX. CONCLUSIONS

The optical and infrared observations of the dwarf novae VW Hyi, 2 days after the return to the quiescent state from a superoutburst, show the presence of a modulation with the superhump period. These observations are consistent with a linear superposition of the normally observed orbital hump modulation plus a late superhump modulation. Because this linear superposition works well, we propose that the orbital and late superhump modulation are unrelated phenomena; these phenomena are likely to occur both in the accretion disk. The late superhump modulation has an almost constant amplitude of ~3 mJy over a wavelength range from just below the Balmer jump till the infrared *K* band. Also, the emission lines peak near the late superhump maximum. These characteristics point to generation of the late superhump light by an optically thin plasma. It is conceivable also that the late superhump modulation is the result of a varying dissipation within the whole disk, e.g., as the result of tidal interaction of the companion star with the disk during the previous superoutburst.

We like to thank S. van Amerongen for providing the mean orbital light curves of VW Hyi in the Walraven passbands.

REFERENCES

Bailey, J., Sherrington, M. R., Giles, A. B., and Jameson, R. F. 1981, *M.N.R.A.S.*, **196**, 121.
Bateson, F. M. 1984, private communication.
Bateson, F. M., and McIntosh, R. 1986, *Pub. Var. Star. Sec. Roy. Astr. Soc. New Zealand*, **13**, 1.
Berriman, G. 1984, *M.N.R.A.S.*, **210**, 223.
Berriman, G., Beattie, D. H., Gatley, I., Lee, T. J., Mochnacki, S. W., and Szkody, P. 1983, *M.N.R.A.S.*, **204**, 1105.
Berriman, G., Szkody, P., and Capps, R. W. 1985, *M.N.R.A.S.*, **217**, 327.
Clarke, C. J., Mantle, V. J., and Bath, G. T. 1985, *M.N.R.A.S.*, **215**, 149.
de Ruiter, H. R., and Lub, J. 1986, *Astr. Ap. Suppl.*, **63**, 59.
Drake, S. A., and Ulrich, R. K. 1980, *Ap. J. Suppl.*, **42**, 351.
Ferland, G. J. 1980, *Pub. A.S.P.*, **92**, 596.
Haefner, R., Schoembs, R., and Vogt, N. 1979, *Astr. Ap.*, **77**, 7.
Hameury, J. M., King, A. R., and Lasota, J. P. 1985, in *Recent Results on Cataclysmic Variables*, (ESA SP-236) p. 167.
Hensler, G. 1985, *Astr. Ap.*, **148**, 423.
Horne, K. 1984, *Nature*, **312**, 348.
Johnson, H. L. 1966, *Ann. Rev. Astr. Ap.*, **4**, 193.
Lub, J., and Pel, J. W. 1977, *Astr. Ap.*, **54**, 137.
Mateo, M., and Szkody, P. 1984, *A.J.*, **89**, 863.
Osaki, Y. 1985, *Astr. Ap.*, **144**, 369.
Papaloizou, J., and Pringle, J. E. 1979, *M.N.R.A.S.*, **189**, 293.
Patterson, J. 1979, *A.J.*, **84**, 804.
———. 1984, *Ap. J. Suppl.*, **54**, 443.
Pringle, J., *et al.* 1987, *M.N.R.A.S.*, **225**, 73.
Rijf, R., Tinbergen, J., and Walraven, Th. 1969. *Bull. Astr. Inst. Netherlands*, **20**, 279.
Schoembs, R. 1986, *Astr. Ap.*, **158**, 233.
Schoembs, R., and Vogt, N. 1980, *Astr. Ap.*, **91**, 25.
———. 1981. *Astr. Ap.*, **97**, 185.
Shafter, A. W., Szkody, P., and Thorstensen, J. R. 1986, *Ap. J.*, **308**, 765.
Sherrington, M. R., Lawson, P. A., King, A. R., and Jameson, R. F. 1980, *M.N.R.A.S.*, **191**, 185.
Smak, J. 1985, *Acta Astr.*, **35**, 1.
van Amerongen, S., Damen, E., Groot, M., Kraakman, H., and van Paradijs, J. 1987, *M.N.R.A.S.*, **225**, 93.
van der Woerd, H., and Heise, J. 1987, *M.N.R.A.S.*, **225**, 141.
van der Woerd, H., Heise, J., and Bateson, F. 1986, *Astr. Ap.*, **156**, 252.
van der Woerd, H., Heise, J., Paerels, F., Beuermann, K., van der Klis, M., Motch, C., and van Paradijs, J. 1987, *Astr. Ap.*, **182**, 219.
Vogt, N. 1974, *Astr. Ap.*, **36**, 369.
———. 1982, *Ap. J.*, **252**, 653.
———. 1983, *Astr. Ap.*, **118**, 95.
Warner, B. 1975, *M.N.R.A.S.*, **170**, 219.
———. 1983, *Inf. Bull. Var. Stars*, No. 2397.
———. 1985, in *Interacting Binaries*, ed. P. Eggleton and J. E. Pringle (Dordrecht: Reidel), p. 367.
Wesemael, F., Auer, L. H., Van Horn, H. M., and Savedoff, M. P. 1980, *Ap. J. Suppl.*, **43**, 159.
Whitehurst, R. 1984, *M.N.R.A.S.*, **207**, 215.
———. 1987, preprint.
Whitehurst, R., Bath, G. T., and Charles, P. A. 1984, *Nature*, **309**, 768.

K. Beuermann: Inst. für Astronomie und Astrophysik, TU Berlin, Hardenbergstrasse 36, D-1000 Berlin 12, Germany

C. Motch: Observatoire de Beçanson, 41 bis av. de l'Observatoire, F-25044, Beçanson, CEDEX, France

M. van der Klis and H. van der Woerd: Exosat Observatory, Space Science Department of ESA, ESTEC-SAE, Keplerlaan 1, 2200 AG Noordwijk, The Netherlands

J. van Paradijs: Astronomical Institute "Anton Pannekoek," University of Amsterdam, Roetersstraat 15, 1018 WB Amsterdam, The Netherlands